

## Double K-shell photoionization of low- $Z$ atoms and He-like ions

J. Hozzowska<sup>1,a</sup>, A.S. Kheifets<sup>2</sup>, M. Berset<sup>1</sup>, I. Bray<sup>5</sup>, W. Cao<sup>1</sup>, J.-Cl. Dousse<sup>1</sup>, K. Fennane<sup>1</sup>, M. Kavčič<sup>4</sup>, Y. Kayser<sup>1</sup>, J. Szlachetko<sup>1,3</sup>, and M. Szlachetko<sup>1</sup>

<sup>1</sup> Physics Department, University of Fribourg, 1700 Fribourg, Switzerland

<sup>2</sup> Research School of Physical Sciences, Australian National University, ACT 0200 Canberra, Australia

<sup>3</sup> European Synchrotron Radiation Facility, 38043 Grenoble, France

<sup>4</sup> J. Stefan Institute, 1001 Ljubljana, Slovenia

<sup>5</sup> ARC Centre for Matter-Antimatter Studies, Curtin University, WA 6845 Perth, Australia

**Abstract.** We report on the investigation of the photon energy dependence of double 1s photoionization of light atoms and compare the cross sections for hollow atom and He-like ion production. Measurements of the  $K\alpha$  hypersatellite x-ray spectra of Mg, Al, and Si were carried out using the Fribourg high-resolution x-ray spectrometer installed at the ID21 and ID26 beam lines at the ESRF. The double-to-single photoionization cross section ratios were derived as a function of the incident photon beam energy and compared to convergent close-coupling (CCC) calculations for He-like ions. The dynamical electron-electron scattering contribution to the DPI cross-sections was found to be more important for neutral atoms than for the He isoelectronic series.

### 1 Introduction

The double photoionization (DPI) process provides a measure of the importance of electron correlations [1]. This is because the single-photon absorption and two-electron ejection is induced by only one single interaction of the photon with the bound electron and it would not occur in the independent electron picture. In atomic structure calculations an accurate theoretical treatment of electron correlations in many-electron systems is still a challenge. Furthermore, the double photoionization process provides insight in fundamental aspects of atomic physics as Breit interaction, quantum electrodynamics (QED) and relativity effects.

The double K-shell ionization of a neutral target leads to a so-called hollow atom, i.e. an atom with an innermost shell empty and outer shells occupied. Since the probability for creating double 1s vacancies by photon impact is quite low ( $\sim 10^{-2}$ – $10^{-6}$ ), experimental data are scarce. With the advent of intense and energy tunable x-ray synchrotron sources hollow atoms have drawn renewed interest on both the experimental and theoretical side. In particular, the investigation of the photon energy dependence of the double 1s vacancy production became accessible. A compilation of the available experimental data for the double-to-single photoionization probability  $P_{KK}$  as a function of the atomic number, including the present work, is shown in Fig. 2. For elements in the range  $10 < Z < 20$ , to the best of our knowledge, the probability for double 1s vacancy production  $P_{KK}$  as a function of the incident photon beam energy has not been determined beforehand. For low- $Z$  atoms the only measurement, performed by means of high-resolution Auger electron spectroscopy, was reported for Ne at a photon energy of 5 keV [2].

<sup>a</sup> e-mail: joanna.hozzowska@unifr.ch

Radiative decay of the 1s double vacancy states yields K x-ray hypersatellite spectra. In fact, Briand et al. [3], in the pioneering work on the K x-ray spectrum of doubly ionized Ga atoms, has identified these shifted in energy x-ray transitions resulting from the decay of doubly ionized states in the same shell and called them *hypersatellites*. In the present work, the double-to-single photoionization cross-section ratios  $P_{KK}$  for Mg, Al, and Si were deduced from the relative intensities of the resolved hypersatellite ( $1s^{-2} \rightarrow 1s^{-1}2p^{-1}$ ) to the diagram ( $1s^{-1} \rightarrow 2p^{-1}$ ) x-ray transitions by employing the high-resolution x-ray emission spectroscopy technique. We have raised the question as to the role of outer shell electrons in the double K-shell photoionization of low-Z atoms. Through a comparison of the photon energy dependence of the K-shell double photoionization cross-sections for hollow atom production to the corresponding DPI cross sections for He-like highly charged counterparts, the influence of outer shell electrons on the electron-electron interactions in the double photoionization process was examined. The double photoionization cross-sections for He-like ions  $Mg^{10+}$ ,  $Al^{11+}$  and  $Si^{12+}$  were calculated within the framework of the convergent close-coupling formalism [4, 5].

## 2 Experiment

The experiments were carried out at two undulator beam lines, ID21 and ID26, at the European Synchrotron Radiation Facility (ESRF), Grenoble, France, by means of high-resolution x-ray spectroscopy employing the Fribourg von Hamos Bragg-type curved crystal spectrometer [6]. The x-ray emission spectra of Mg were measured using a TiAP(001) crystal ( $2d = 25.772 \text{ \AA}$ ) in second order and those of Al and Si with an ADP(101) ( $2d = 10.642 \text{ \AA}$ ) crystal in first order. The diffracted x-rays were recorded with a 26.8 mm long and 8 mm high position-sensitive back-illuminated CCD (charged coupled device) camera consisting of 1340 columns and 400 rows with a pixel size of  $20 \times 20 \mu\text{m}^2$ . The CCD detector was cooled down thermo-electrically to  $-50^\circ\text{C}$ . Self-supported  $3.3 \mu\text{m}$  and  $50 \mu\text{m}$  thick metallic foils of Mg,  $1 \mu\text{m}$  thick foil of Al and a 1 mm thick c-Si sample were used. The energy calibration and the instrumental response of the crystal spectrometer were determined from the measurements of the  $K\alpha$  x-ray lines of Mg, Al and Si, and the  $L\beta_1$  lines of Se and Ag with reference energy values from [7] and natural line widths from [8]. The instrumental response function of the spectrometer was found to be well reproduced by a Lorentzian profile with a width (FWHM) of  $0.54(1) \text{ eV}$  at the energy of the Mg K-hypersatellite line and a Gaussian profile width (FWHM) of  $0.32(1) \text{ eV}$  and  $0.40(1) \text{ eV}$  for the Al and Si K-hypersatellite line, respectively. At the ID21 beam line monochromatic photon beams with a 10 eV bandpass were obtained using two  $20 \text{ \AA}$  Ni( $B_4C$ ) multilayers and residual upper harmonics were suppressed with a Ni mirror. The beam size was defined by means of a 1 mm in diameter pinhole. A slit width of 0.2 mm was used as the best compromise between an acceptable energy resolution and the detection efficiency. At the ID26 beam line the double-crystal Si(111) monochromator was employed and the Si coated and Cr coated double mirrors were used for harmonic rejection. The beam was focused horizontally to  $\sim 250 \mu\text{m}$  at the sample thereby permitting to operate the spectrometer in the so-called slit-less geometry leading to a higher overall detection efficiency. The incident photon flux was  $\sim 1-3 \times 10^{12} \text{ ph/s}$  on both beam lines.

The high-resolution K-hypersatellite x-ray emission spectra of Mg and Si at are shown in Fig. 1. For light elements only the  $K\alpha_2^h$  hypersatellite ( $^1P_1 \rightarrow ^1S_0$ ) is observed, the spin-flip  $K\alpha_1^h$  transition ( $^3P_1 \rightarrow ^1S_0$ ) being forbidden by the E1 selection rule in the L-S coupling scheme that prevails for low-Z elements. The K-hypersatellite x-ray emission line is accompanied by L-satellites resulting from the presence of the 2p and 2s vacancies during the x-ray transition. In addition, on the low energy side of the  $K\alpha_2^h$  x-ray spectra the  $K\beta L^2(K^{-1}L^{-2} \rightarrow L^{-2}M^{-1})$  and the  $K\beta L^1(K^{-1}L^{-1} \rightarrow L^{-1}M^{-1})$  satellite transitions can be seen for Mg and Si, respectively. To deduce the intensities of the K-hypersatellite lines the measured spectra of Mg were fitted with Lorentzian profiles and those of Al and Si with Voigt functions. The obtained x-ray line intensities were corrected for the sample self-absorption and absorption of the incident x-rays, the photon flux, the spectrometer solid angle, as well as for the CCD detector quantum efficiency.

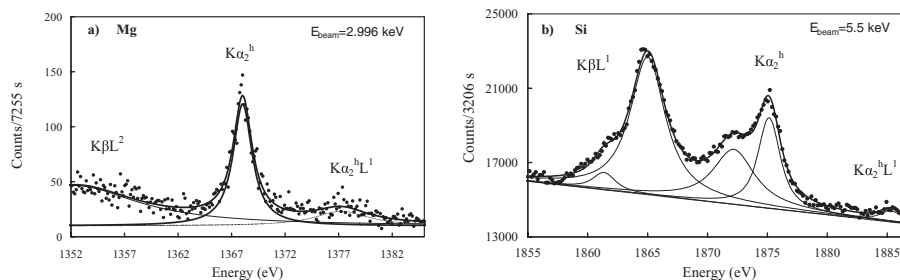


**Fig. 1.** High-resolution K-hypersatellite x-ray emission spectra of Mg (a) and Si (b) measured at photon energies close to the maximum of the DPI cross sections.  $K\alpha_2^h$  hypersatellite transition energies of 1367.86(6) eV for Mg and 1874.87(4) eV for Si were found.

### 3 Results and discussion

Following the single photon absorption, the double ionization proceeds via electron-electron interaction. Two dominant mechanisms, namely the shakeoff (SO) and the electron inelastic scattering (so-called knock-out KO or two-step-one TS1) contribute to the double K-shell photoionization. In the shake process the primary electron is ejected rapidly and due to a sudden change of the atomic potential a subsequent removal of the remaining electron to the continuum or to a bound state takes place. The double K-shell photoionization via shake is a consequence of the change in the self-consistent field and electron-electron correlations. In the case of TS1, the outgoing photoelectron knocks out the second one in an (e,2e) like electron impact half-collision. The initial-state correlations are important in shakeoff, while the final-state electron interactions are essential for the electron scattering TS1.

The photon energy dependence of the TS1 and the SO processes differ. Shake prevails at high photon energies, while TS1 dominates at low and intermediate excitation energies to become negligible in the photoabsorption asymptotic regime where the double-to-single photoionization ratio approaches a constant value. To probe the evolution of the double ionization probability with the photon energy, the  $K\alpha^h$  x-ray transitions were measured at different incident beam energies from 2.746 keV to 8.000 keV for Mg, from 3.122 keV to 7.000 keV for Al, and from 3.600 keV to 10.000 keV for Si. The ratios of the double-to-single K-shell ionization by photoabsorption  $P_{KK}$  and the DPI cross-sections  $\sigma^{2+}$  were determined from the relative intensities  $I$  of the measured  $K\alpha_2^h$  and  $K\alpha$  x-ray emission lines employing the expressions:  $P_{KK} = \frac{\omega_K I_{K\alpha^h}}{\omega_{KK} I_{K\alpha}}$  and  $P_{KK} = \frac{\sigma^{2+}}{\sigma^+}$ , where  $\omega_K$  and  $\omega_{KK}$  are the fluorescence yields for the single- and double-hole state [9], respectively, and  $\sigma^+$  stands for the single K-shell photoionization cross section from [10]. The double to single K-shell photoionization ratios in the peak region of the photon energy evolution  $P_{KK}^{max}$  were determined to be  $2.02(11) \times 10^{-3}$  for Mg,  $1.78(12) \times 10^{-3}$  for Al and  $1.43(8) \times 10^{-3}$  for Si. The experimental results are represented in Fig. 2 along with the data for other elements, the power law fit from [11] and the Z-scaling laws for He-like ions. In fact, to plot the trend of the  $P_{KK}$  in the peak region as a function of Z was first suggested by Kanter et al. [12]. A significantly larger electron scattering contribution in heavy atoms compared to low-Z elements was evinced and a weaker  $1/Z^{1.6}$ -dependence than the  $1/Z^2$  fall-off for shake-off of the double photoionization probability  $P_{KK}^{max}$  was established [11]. Our results for the double-to-single photoionization cross section ratios of Mg, Al, and Si are in good agreement with the  $1/Z^{1.6}$ -dependence of the  $P_{KK}^{max}$  for neutral atoms. However, compared to the calculated  $P_{KK}^{max}$  values for two-electron targets of  $1.23 \times 10^{-3}$  for  $Mg^{10+}$ ,  $1.10 \times 10^{-3}$  for  $Al^{11+}$  and  $9.37 \times 10^{-4}$  for  $Si^{12+}$ , they lie systematically higher. The same holds for the values of the DPI cross sections  $\sigma^{2+}$  as illustrated in Fig. 3. For the helium isoelectronic sequence the shake-off (SO) ratio in the high-energy limit can be calculated quite accurately provided that electron correlation when one electron is close to the nucleus is accounted for in the initial state wave function [13–15]. The double-to-single ratio in the asymptotic limit can be also deduced from the double K-shell ionization following nuclear electron capture (EC). As shown in Fig. 2, both the theoretical predictions for SO and the EC radioactive source measurements are in good agreement. In a recent

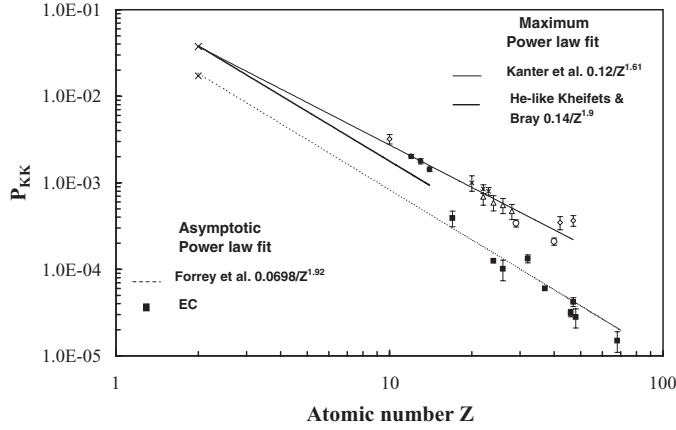


**Fig. 2.** The ratio of double to single K-shell photoionization versus the atomic number. • Present results, \* [22], ○ [25,26], △ [23], ◇ [11], × [18,24], and EC (electron capture) [27]. For He-like ions the  $P_{KK}^{max}$  are from Kheifets and Bray [4] and this work (thick solid line). The photoabsorption asymptotic limits of Forrey et al. (dashed line) [15] are also shown.

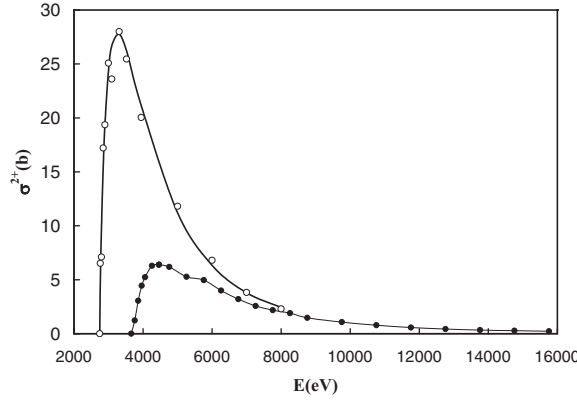


**Fig. 3.** The double K-shell photoionization cross sections  $\sigma^{2+}$  as a function of the photon energy for Mg ○ experimental results, and Mg<sup>10+</sup> ● present CCC calculations in the velocity gauge.

work [16] on correlated wave functions for the K-shell electrons of neutral atoms and helium-like atoms it was found that the influence of passive outer shell electrons on electron-electron correlation is very small. The outer shell electrons affect the electron-nucleus interaction but not the electron-electron interaction. Thus, it is plausible to assume that the photoabsorption asymptotic shake-off values for the He-like ions and neutral atoms are almost the same. Since the TS1 term predominates in the broad maximum of the  $P_{KK}$  because of the different photon energy dependence of the TS1 and the SO processes, the observed higher values of  $P_{KK}^{max}$  for neutral atoms indicate that the electron scattering contribution to DPI is more important than for He-like ions. This finding is related to the proportionality of electron-impact ionization of a hydrogen-like ion to the TS1 term of the double photoionization of the same He-like atom [17–21].

In conclusion, the comparison of our results with other experimental data and theory confirms the importance of the final-state electron-electron interaction term TS1 to the double 1s photoionization probability for Mg, Al and Si. The effect of outer shell electrons on the double K-shell photoionization in neutral low- $Z$  atoms is primarily reflected in the electron scattering contribution due to the change of the effective nuclear charge. Calculations of the double photoionization cross sections for neutral atoms would certainly shed new light on the electron-electron interactions.

The financial support of the Swiss National Science Foundation is acknowledged. The authors would like to thank the ESRF for support, in particular Dr. D. Reichert and Dr. R. Tucoulou from the ID21 beam line and Dr. Tsu Chien Weng from the ID26 beam line.

## References

1. J.H. McGuire, *Electron Correlation and Dynamics in Atomic Collisions* (Cambridge University Press, Cambridge, UK, 1997)
2. S.H. Southworth, et al., *Phys. Rev. A* **67**, 062712 (2003)
3. J.P. Briand, et al., *Phys. Rev. Lett.* **27**, 777 (1971)
4. A.S. Kheifets, I. Bray, *Phys. Rev. A* **58**, 4501 (1998)
5. A.S. Kheifets, I. Bray, *Phys. Rev. A* **75**, 042703 (2007)
6. J. Hozzowska, et al., *Nucl. Instrum. Meth. Phys. Res. A* **376**, 129 (1996)
7. R.D. Deslattes, et al., *Rev. Mod. Phys.* **75**, 35 (2003)
8. J.L. Campbell, T. Papp, *At. Data Nucl. Data Tables* **77**, 1 (2001)
9. M.H. Chen, *Phys. Rev. A* **44**, 239 (1991)
10. <http://physics.nist.gov/PhysRefData/Xcom/Text/XCOM.html>
11. E.P. Kanter, et al., *Phys. Rev. A* **73**, 022708 (2006)
12. E.P. Kanter, et al., *Phys. Rev. Lett.* **83**, 508 (1999)
13. T. Pattard, et al., *J. Phys. B: At. Mol. Opt. Phys.* **36**, L189 (2003)
14. M.A. Kornberg, J.E. Miraglia, *Phys. Rev. A* **49**, 5120 (1994)
15. R.C. Forrey, et al., *Phys. Rev. A* **51**, 2112 (1995)
16. D.M. Mitnik, J.E. Miraglia, *J. Phys. B: At. Mol. Opt. Phys.* **38**, 3325 (2005)
17. J.A.R. Samson, et al., *Phys. Rev. Lett.* **65**, 2861 (1990)
18. J.A.R. Samson, et al., *Phys. Rev. A* **57**, 1906 (1998)
19. A.S. Kheifets, *J. Phys. B: At. Mol. Opt. Phys.* **34**, L247 (2001)
20. T. Schneider, J.-M. Rost, *Phys. Rev. A* **67**, 062704 (2003)
21. T. Pattard, J. Burgdörfer, *Phys. Rev. A* **64**, 042720 (2001)
22. M. Oura, et al., *J. Phys. B: At. Mol. Opt. Phys.* **35**, 3847 (2002)
23. J. Ahopelto, *Phys. Scr.* **20**, 71 (1979)
24. L. Spielberger, et al., *Phys. Rev. Lett.* **74**, 4615 (1995)
25. R. Diamant, et al., *Phys. Rev. A* **62**, 052519 (2000)
26. S. Huotari, et al., *J. Elec. Spec. Relat. Phenom.* **137**, 293 (2004)
27. A. Suzuki, J. Law, *Phys. Rev. C* **25**, 2722 (1982)